Original Article

Inactivated Sendai Virus Induces Apoptosis Mediated by Reactive Oxygen Species in Murine Melanoma Cells*

GAO Hui[1,2], LI Ling Yu[2], ZHANG Man[1], and ZHANG Quan[2,#]

1. College of Clinical Medicine of Yangzhou University, Yangzhou 225001, Jiangsu, China; 2. Jiangsu Co-innovation Center for Prevention and Control of Important Animal Infectious Diseases and Zoonoses, College of Veterinary Medicine, Yangzhou University, Yangzhou 225009, Jiangsu, China

Abstract

Objective This paper aims to investigate the apoptotic effect of inactivated Sendai virus (hemagglutinating virus of Japan-enveloped, HVJ-E) on murine melanoma cells (B16F10) and the possible mechanisms involved in the putative apoptotic reactions.

Methods B16F10 cells were treated with HVJ-E at various multiplicities of infection (MOI), and the reactive oxygen species (ROS), cell viability, and apoptosis were measured. Next, the roles of ROS in the regulation of Bcl-2/Bax and the activation of mitogen-activated protein kinase (MAPK) pathways in HVJ-E-treated B16F10 cells were analyzed. To further evaluate the cytotoxic effect of HVJ-E-generated ROS on B16F10 cells, HVJ-E was intratumorally injected, both with and without N-acetyl-L-cysteine (NAC), into melanoma tumors on BALB/c mice. Tumor volume was then monitored for 3 weeks, and the tumor proteins were separated for immunoblot assay.

Results Treatment of B16F10 cells with HVJ-E resulted in a dose-dependent inhibition of cell-viability and an induction of apoptosis. The latter effect was associated with the generation of ROS. Inhibition of ROS generation by NAC resulted in a significant reduction of HVJ-E-induced Erk1/2, JNK, and p38 MAPK activation. Additionally, ROS inhibition caused a decrease in the Bcl-2/Bax ratio as well as promoting activation of apoptosis both *in vitro* and *in vivo*.

Conclusion These results suggest that HVJ-E possesses potential anticancer activity in B16F10 cells through ROS-mediated mitochondrial dysfunction involving the MAPK pathway.

Key words: Inactivated Sendai virus (HVJ-E); Reactive oxygen species; MAPK; Apoptosis

Biomed Environ Sci, 2016; 29(12): 877-884 *doi: 10.3967/bes2016.117* *ISSN: 0895-3988*

www.besjournal.com (full text) *CN: 11-2816/Q*

INTRODUCTION

Oncolytic viruses are used in new cancer therapeutic approaches that exhibit great potential. Recently, inactivated Sendai virus particles (hemagglutinating virus of Japan-envelope, HVJ-E) obtained *via* UV irradiation, which are widely recognized for their ability to elicit multiple anti-tumor immune responses[1-3], were also shown to kill cancer cells directly by inducing apoptosis[4-6]. Previous studies have demonstrated that HVJ-E-activated mitogen-activated protein kinase (MAPK) pathway, resulting in the subsequent induction of apoptosis in a variety of cancer cells[4,7].

*This work was supported by the National Natural Science foundation of China (No.31302042); the Natural Science Foundation of Jiangsu Province (BK20130445); the Priority Academic Program Development of Jiangsu Higher Education Institutions, and the Young and Middle-aged Academic Leaders Plan of Yangzhou University.

#Correspondence should be addressed to Dr. ZHANG Quan, E-mail: zquan@yzu.edu.cn

Biographical note of the first author: GAO Hui, PhD, female, born in 1961, associate professor, major in dermatology medicine.

However, the mechanisms by which HVJ-E activates MAPK pathway in cancer cells remain to be elucidated.

MAPKs are serine-threonine protein kinases that play an important role in the regulation of many cellular processes, including cell growth and proliferation, differentiation, and apoptosis. Canonical MAPKs are classified into three major components: p38, Erk1/2, and JNK, all of which have been reported to be involved in apoptosis[8]. Previous studies have indicated that reactive oxygen species (ROS) have the capacity to induce or mediate the activation of MAPK pathways[9]. Additionally, the activation of Erk1/2, JNK, and p38 MAPK signaling proteins have been observed to be involved in apoptosis following ROS generation[10-12]. However, very few studies have addressed the role of ROS in the regulation of MAPK activation following HVJ-E exposure.

In the present study, we report for the first time that HVJ-E-induced MAPK activation and subsequent apoptosis are associated with ROS generation. Further analysis in B16F10 cells suggests that inhibition of ROS generation by treatment with N-acetyl-L-cysteine (NAC) prevents HVJ-E-induced apoptosis by inhibiting the phosphorylation of JNK, p38, and Erk1/2. NAC treatment also resulted in a decrease in the Bcl-2/Bax ratio. Collectively, our data provide new insights into the mechanisms that underpin HVJ-E-induced apoptosis in tumor cells.

MATERIALS AND METHODS

Cells, Virus, and Mice

The murine melanoma cell line, B16F10, was purchased from the Cell Bank at the Chinese Academy of Science (Shanghai, China). Cells were cultured in RPMI 1640 supplemented with 10% fetal bovine serum. Sendai virus was harvested from the chorioallantoic fluid from 10-14 day-old chick eggs, purified by centrifugation, and inactivated by UV irradiation (99 mJ/cm^2), as previously described[13]. BALB/c mice (5 weeks old) were purchased from the Experimental Animal Center of Yangzhou University. All animal procedures were performed in compliance with the animal experimentation guidelines of Yangzhou University.

Antibodies and Reagents

Antibodies against the following proteins were used: caspase-3 (9664), Bax (2772), Bcl-2 (2870), p53 (2524), phospho-JNK (4668), phospho-p38 (4511), phospho-Erk1/2 (4370), total p38 (9212), total JNK (9252), total Erk1/2 (4695), poly (ADP-ribose) polymerase (PARP) (9542), and β-actin (4970). The antibodies were purchased from Cell Signaling Technology. Horseradish peroxidase (HRP)-conjugated anti-rabbit goat immunoglobulin (sc-2004) was obtained from Santa Cruz Biotechnology. NAC was purchased from Sigma-Aldrich (A7250). The FITC Annexin V Apoptosis Detection Kit I was purchased from BD Biosciences.

Cellular Morphological Changes

Changes in the morphology of cells that had been treated with each indicated mutiplicites of infection (MOI) of HVJ-E for 24 h were photographed using an inverted microscope (DMI 3000B, Leica).

Measurement of Intracellular ROS

Intracellular ROS were measured using 2',7'-dichlorofluorescein diacetate (DCFH-DA, Beyotime, Shanghai, China). A total of 5×10^5 B16F10 cells were either mock-treated (PBS) or treated with HVJ-E at a MOI of 500, 1000, or 1500. To verify if ROS generation is related to HVJ-E-induced cellular apoptosis, some cells were treated with NAC, an ROS scavenger. To perform this assay, B16F10 cells were incubated with NAC (100 μmol/L) for 30 min prior to HVJ-E (1500 MOI) treatment. Collected cells were analyzed by flow cytometry.

Cell Viability Assay

Cell viability was determined using CCK-8 assays (Beyotime, Shanghai, China). Briefly, cells were seeded into 96-well plates at a density of 1×10^4 cells per well and incubated for 24 h. After treatment according to the various experimental conditions, 20 μL of kit reagent was added to each well, and the cells were incubated for an additional 4 h. The optical density (OD) at 450 nm was recorded using a Bio-Tek ELISA microplate reader. The cell viability rate was determined by calculating the ratio of the OD of the experimental wells to that of the normal wells.

The Analysis of Apoptosis Using Flow Cytometry

Apoptosis was observed by analyzing the membrane redistribution of phosphatidylserine using flow cytometry with the annexin V and propidium iodide (PI) double-staining technique, as

previously described[4]. A total of 5 × 10^5 B16F10 cells were either mock-treated or treated with HVJ-E at a MOI of 500, 1000, or 1500, and the percentage of apoptotic cells was determined. For the apoptosis inhibition assays, the B16F10 cells were incubated with NAC (100 μmol/L) for 30 min prior to HVJ-E treatment at 1500 MOI. Apoptosis was then measured and compared to the cells not treated with NAC at the indicated MOI.

Western Blotting Analysis

Cells or transplanted tumors, which were treated using the conditions indicated above, were homogenized in a radio immunoprecipitation assay (RIPA) buffer containing a protease inhibitor cocktail. 30 μg of protein was separated using 10%-15% SDS-PAGE and transferred to PVDF membranes. After blocking with 5% non-fat milk for 2 h, the membranes were incubated overnight with the appropriate primary antibodies at 4 °C. The immunoreactive bands were visualized using enhanced chemiluminescence after the membranes had been incubated with HRP-conjugated IgG secondary antibodies.

In Vivo Oncolysis

BALB/c mice were randomly divided into four groups, with each group consisting of eight mice. B16F10 cells (1 × 10^6) were injected into the backs of the mice. Treatment was initiated on day 7, when the diameter of the tumor had reached approximately 5 mm. The various treatments were performed on one of the four groups: treatment with PBS, treatment with HVJ-E (1 × 10^{10} particles), treatment with NAC only (100 μmol/L), and treatment with NAC plus HVJ-E. Tumor growth was observed on a daily basis, and tumor volume was measured at 2-day intervals in a blinded manner with slide calipers using the following formula: tumor volume (mm^3) = length × $(width)^2/2$[4].

Statistical Analysis

For all experiments, statistical analyses were first performed using one-way analysis of variance (ANOVA) to determine the statistically significant variation among the groups for each endpoint that was assessed. Multiple comparisons between treatment and control groups were then performed using Dunnett's LSD tests. Differences with a value of $P < 0.05$ were considered to be significant.

RESULTS

HVJ-E Induces ROS Generation and Apoptosis in B16F10 Cells

To assess whether HVJ-E induces ROS generation in murine melanoma cells *in vitro*, B16F10 cells were treated with the indicated MOIs of HVJ-E for 24 h. As shown in Figure 1A and 1B, the level of ROS that were generated increased in B16F10 cells in response to HVJ-E treatment in a dose-dependent manner, which suggests that HVJ-E induced ROS accumulation in B16F10 cells. The changes in cellular morphology and the results of the CCK-8 assay analysis demonstrated that HVJ-E reduced the cell viability in a dose-dependent manner compared to the controls (Figure 1C and 1D). Next, we sought to determine whether this reduced cell viability was due to the induction of apoptosis by analyzing annexin-V/PI double staining in cells treated with HVJ-E. A significant increase in apoptosis was observed in B16F10 cells treated with HVJ-E in a dose-dependent manner, which further suggests that HVJ-E exerted an oncolytic effect in B16F10 cells (Figure 1E and 1F). Taken together, these results suggest that HVJ-E induced both ROS generation and apoptosis in B16F10 cells.

HVJ-E Decreases the Bcl-2/Bax Ratio and Activates MAPK Signaling Pathways

It has been suggested that the Bcl-2 protein family is regulated by p53 and is involved in the inhibition of apoptosis[14-15]. To determine whether HVJ-E regulates p53 and Bcl-2 signaling in B16F10 cells, we monitored the expression of p53, Bcl-2, and Bax, following HVJ-E treatment. The results showed that p53 was significantly activated upon HVJ-E treatment in B16F10 cells (Figure 2A and 2C). Additionally, HVJ-E treatment alone caused a significant decrease in the expression of the anti-apoptotic protein, Bcl-2. The same treatment resulted in a dramatic increase in the levels of the pro-apoptotic protein, Bax. Consequently, this resulted in a dramatic decrease in the Bcl-2/Bax ratio (Figure 2A and 2B). In addition, as shown in Figure 2D, HVJ-E treatment significantly stimulated the phosphorylation of Erk1/2, JNK, and p38 MAPK, while simultaneously resulting in the cleavage of caspase-3 and PARP, which are both required for the execution of apoptosis (Figure 2D). Together, these data suggest that HVJ-E activates p53, while decreasing the Bcl-2/Bax ratio and activating

downstream MAPK signaling pathways.

HVJ-E-induced Apoptosis in B16F10 Cells is ROS Dependent

It has been reported that ROS regulate the expression of Bcl-2 and Bax[16]. To evaluate the role of ROS in HVJ-E-induced apoptosis in B16F10 cells, the cells were treated with an ROS scavenger, NAC, prior to HVJ-E treatment. The results revealed that NAC not only blocked ROS generation (Figure 3A and 3B), but also significantly inhibited HVJ-E-induced apoptosis (Figure 3C and 3D). Additionally, an increase in both cell viability and the Bcl-2/Bax ratio were observed following NAC treatment compared with HVJ-E-treated cells, and HVJ-E-induced p53 expression was inhibited following NAC treatment (Figure 3E-3H). Furthermore, the results suggested that NAC treatment protected B16F10 cells from HVJ-E-induced activation of p38, JNK, Erk1/2, and cleavage of caspase-3 (Figure 3I). These results further suggest that the Bcl-2 family and the MAPK pathways play a role downstream of ROS during the regulation of B16F10 cellular apoptosis.

HVJ-E Acts as an Effective Oncolytic Agent in Vivo

Since our data demonstrated that HVJ-E induced

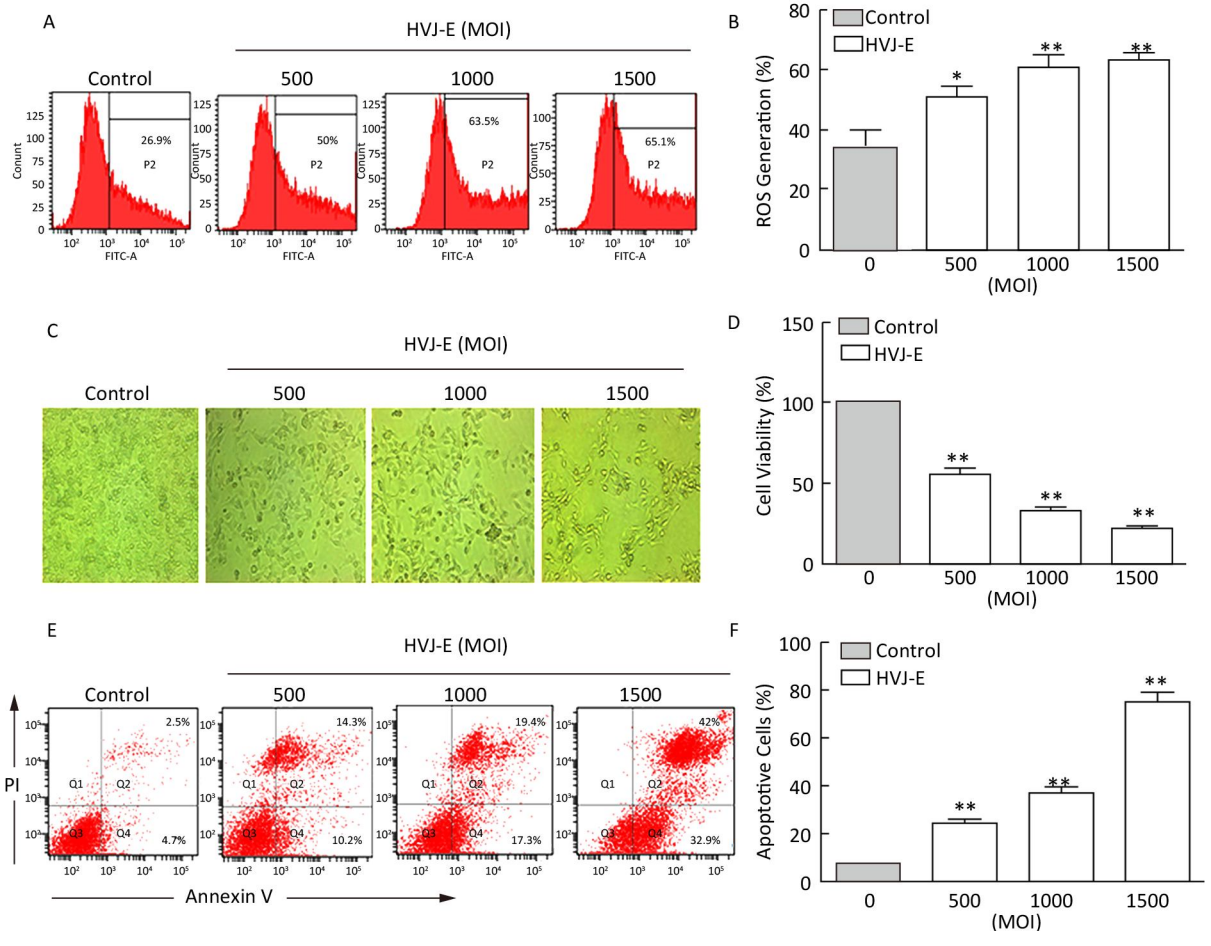

Figure 1. HVJ-E induces ROS and apoptosis in B16F10 cells. (A, B) Cells were treated with HVJ-E at the indicated MOI for 24 h, and the intracellular ROS were detected using the DCF-DA method. Data are presented as mean ± SD following three experiments performed four times. (C) Cells were treated with HVJ-E at the indicated MOI for 24 h, and cell morphology was observed under a microscope. (D) The effect of HVJ-E at the indicated MOI on B16F10 cell viability, as assessed using CCK-8 assays. Data are presented as means ± SDs following three experiments performed four times. (E, F) B16F10 cells were either mock- or HVJ-E-treated at an MOI of 500, 1000, and 1500 for 24 h. Cells were then harvested, double-stained with annexin V and propidium iodide (PI), and analyzed using flow cytometry. The data are presented as the mean ± SD following three independent experiments. $^{**}P < 0.01$ *vs.* control cells. $^{*}P < 0.05$ *vs.* control cells.

ROS-dependent cellular apoptosis and death in B16F10 cells *in vitro*, we next asked whether HVJ-E has a similar effect *in vivo*. As illustrated in Figure 4A, the results revealed that HVJ-E significantly inhibits melanoma tumor growth compared with the PBS-treated group. Additionally, NAC dramatically abolishes the tumor inhibition effect induced by HVJ-E. To further investigate this phenomenon, tumor proteins were isolated and subsequently detected by Western blot analysis. The results demonstrated that NAC inhibits the HVJ-E-induced activation of p53 and the HVJ-E-induced reduction of the Bcl-2/Bax ratio (Figure 4B-4D). NAC also inhibited HVJ-E-induced effects on JNK, p38, Erk 1/2, and caspase-3 (Figure 4E), which were consistent with results obtained from the *in vitro* experiments. Collectively, these results suggest that ROS generation is a function of cellular apoptotic mechanisms induced in HVJ-E-treated B16F10 cells.

DISCUSSION

HVJ-E is considered to be a safe and efficient non-pathogenic vector that can potentially be used for cancer therapy by facilitating immune-mediated reactions and inducing apoptosis against malignancy. A protocol for a phase I/IIa clinical study into the use of HVJ-E in malignant melanoma was approved in 2009 by the ethics committees of Osaka University and the Medical Center for Translational Research in

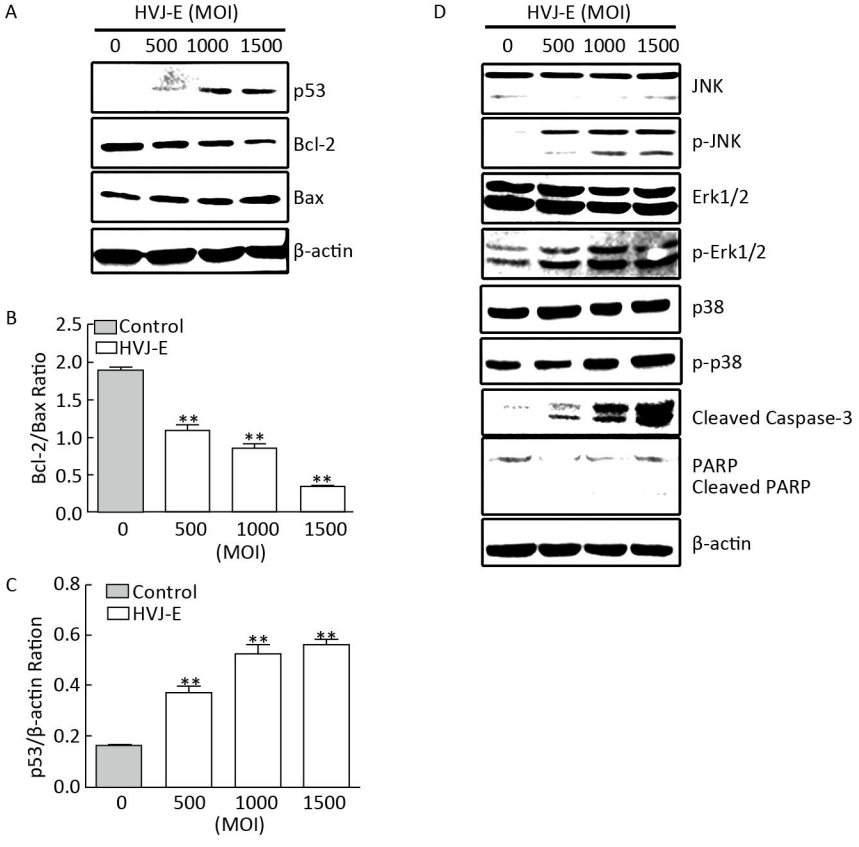

Figure 2. HVJ-E treatment causes a decrease in the Bcl-2/Bax ratio and activates MAPK pathways in B16F10 cells. B16F10 cells were either mock- or HVJ-E-treated at the indicated MOI. Cell lysates were analyzed using Western blotting with specific antibodies against molecules that perform roles in apoptotic pathways. (A) The expression levels of p53, Bcl-2, and Bax; β-actin was used as a loading control. (B, C) Blots for p53, Bcl-2, and Bax in B16F10 cells were semi-quantified using Image Lab™ software. Data are expressed as mean ± SD (n = 3) relative to control. ** $P < 0.01$ in comparison to the control following one-way ANOVA. (D) B16F10 cells were treated as described in Figure 2A, and MAPK activation was examined using specific antibodies against phosphorylated Erk1/2, JNK, and p38. The expression of the total protein levels was measured and used as a loading control.

Osaka University Hospital[17]. The study resulted in significant progress for determining the effects of HVJ-E-mediated therapeutics. However, the underlying mechanisms that result in these effects remain largely unclear.

In our previous study, we demonstrated that HVJ-E induced the activation of MAPKs, including JNK, p38, MAPK, and Erk1/2 MAPK[4]. However, the precise mechanisms underlying MAPK activation caused by HVJ-E are unclear. The most important findings in relation to this study were that reduced cell viability and the induction of apoptosis that was observed after HVJ-E treatment were associated with ROS generation. These effects were most likely the result of MAPK activation and apoptosis induction.

ROS are oxygen-derived free radicals[18]. Low levels of ROS have been observed to moderately promote cell proliferation. Relatively high levels of ROS can induce cellular apoptosis, and even higher levels of ROS have been suggested to cause cell necrosis[19]. Following the continuous oxidative stress effect associated with ROS, cancer cells with higher levels of ROS have been observed to die more

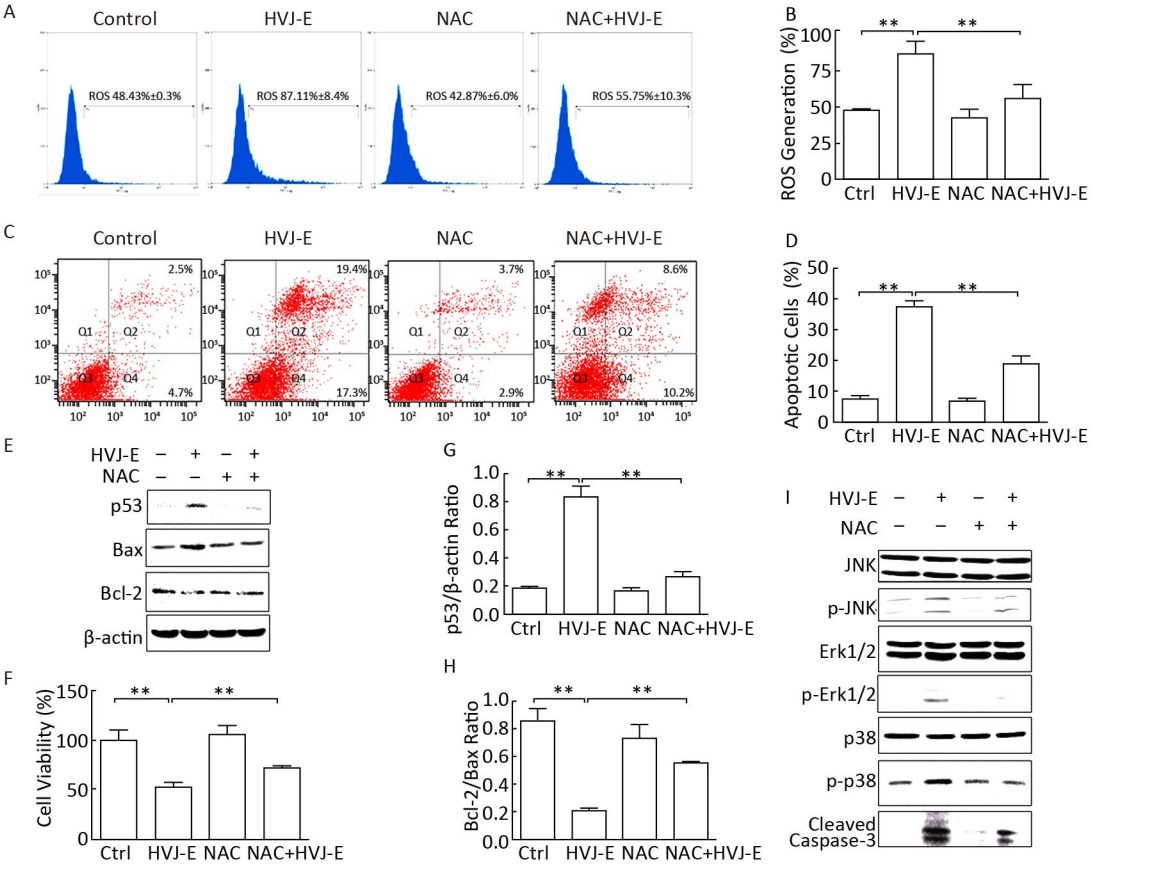

Figure 3. ROS scavenger, NAC, abolishes HVJ-E-induced apoptosis. (A, B) Cells were either mock-treated or pretreated with NAC (100 μmol/L). These cells were subsequently treated with HVJ-E (MOI = 1000). The intracellular ROS were detected using the DCF-DA method. Data are presented as mean ± SD following three experiments performed four times. (C, D) Cells were treated as described above, and cellular apoptosis was measured using flow cytometry. The data show the mean ± SDs for three experiments. (E-H) The expression levels of p53, Bcl-2, and Bax; cells were treated as described above; β-actin was used as a loading control. Western blots of p53, Bcl-2, and Bax levels in B16F10 cells were semi-quantified using Image Lab™ software. Data are expressed as mean ± SD (n = 3) relative to control. All experiments were performed twice. (I) MAPK activation was examined using specific antibodies against phosphorylated Erk1/2, JNK, and p38 (B16F10 cells were treated as described above). The expression of the total protein levels was measured and used as a loading control. $^{**}P < 0.01$ *vs.* control cells.

quickly than normal cells. Therefore, tumor cells that are highly sensitive to ROS have been used to explore new antitumor drugs, with the hope of identifying new clinical compounds displaying good efficacy and low toxicity[20-21]. Evidence has shown that both Sendai virus and UV-inactivated Sendai virus may induce oxidative stress in Madin-Darby canine kidney cells[22]. However, whether HVJ-E has an effect similar to the live virus on cancer cells remains unknown. In the current study, the production of intracellular ROS was significantly increased in a dose-dependent manner when treated with HVJ-E for 24 h (Figure 1A), which demonstrated that HVJ-E could lead to the accumulation of intracellular ROS in cancer cells.

Bcl-2 family members constitute a complex network that participates in the regulation of apoptosis. These proteins are recognized as potential targets in the treatment of tumors[23]. It has been reported that ROS generation affects the expression of Bcl-2 and Bax[24]. When the ratio of Bcl-2/Bax is low, there is a tendency towards an increase in cellular apoptosis; when it is high, cellular apoptosis will tend to decrease. The results of western blotting analysis showed that, following treatment of B16F10 cells with HVJ-E, the expression of the anti-apoptotic protein, Bcl-2, decreased. Conversely, the expression of the pro-apoptotic protein, Bax, increased. This resulted in a decrease in the Bcl-2/Bax ratio. Therefore, it can be concluded that proteins of the Bcl-2 family are involved in the regulation of HVJ-E-induced apoptosis in B16F10 cells.

It has been reported that respiratory virus infection can induce ROS generation and activate MAPK pathways in multiple cell types[22,25]. Therefore,

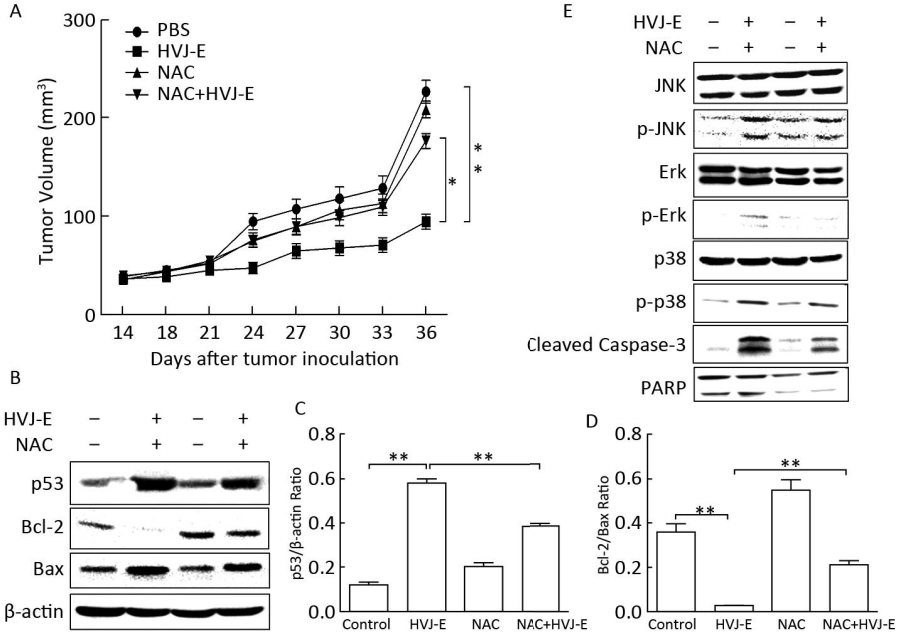

Figure 4. NAC abolishes the HVJ-E-induced tumor growth inhibition in BALB/c mice. (A) BALB/c mice bearing B16F10 tumors were treated with PBS, NAC, HVJ-E or co-injection of NAC and HVJ-E. At 10 d post-treatment, two mice were sacrificed, and tumors were processed for western blotting analysis. (A) Tumor volumes were measured at 2-day intervals for 21 d and expressed as the mean ± SD (n = 6) using tumor volume/time curves. The difference in tumor regression was significant between the HVJ-E and B16F10 control group (P < 0.001) and between the HVJ-E and NAC+HVJ-E group (P < 0.05). (B) Expression levels of p53, Bcl-2, and Bax; β-actin was used as a loading control. (C, D) Blots for p53, Bcl-2, and Bax in B16F10 cells were semi-quantified using Image Lab™ software. Data are expressed as mean ± SDs (n = 3) relative to control. $^{**}P$ < 0.01 in comparison to the control following one-way ANOVA. (E) MAPK activation and cleavage of caspase-3 were examined using specific antibodies against phosphorylated Erk1/2, JNK, and p38. The expression of the total protein levels was measured and used as a loading control.

we examined the possibility that MAPK pathways are involved in HVJ-E-induced cellular apoptosis in B16F10. The results showed that HVJ-E activated p38, Erk1/2, and JNK in B16F10 cells, resulting in the cleavage of caspase-3 and PARP (Figure 2).

To clarify further the relationship between ROS and HVJ-E-induced apoptosis in B16F10 cells, some cells were pre-treated with NAC prior to HVJ-E treatment. When compared to cells that had not been pre-treated with NAC, we observed that NAC treatment significantly altered the relative levels of cleaved caspase-3, Bcl-2, Bax, p-JNK, p-p38, and p-Erk1/2. This demonstrated that NAC significantly reversed HVJ-E-induced apoptosis in B16F10 cells both *in vitro* and *in vivo*, and thereby confirmed the role of ROS in the process of HVJ-E-induced apoptosis in B16F10 cells.

To summarize our analysis, we demonstrated that the apoptosis-inducing potential of HVJ-E was related to its ROS production. When ROS were scavenged by incubation with the antioxidant NAC, HVJ-E-induced apoptosis was markedly suppressed. These results provide a novel insight into the underlying mechanisms for the anti-tumor effects of HVJ-E.

Received: May 31, 2016;
Accepted: November 20, 2016

REFERENCES

1. Zhang Q, Yuan WF, Zhai GQ, et al. Inactivated Sendai virus suppresses murine melanoma growth by inducing host immune responses and down-regulating beta-catenin expression. Biomed Environ Sci, 2012; 25, 509-16.
2. Kurooka M, Kaneda Y. Inactivated Sendai virus particles eradicate tumors by inducing immune responses through blocking regulatory T cells. Cancer Res, 2007; 67, 227-36.
3. Saga, K, Tamai K, Yamazaki T, et al. Systemic administration of a novel immune-stimulatory pseudovirion suppresses lung metastatic melanoma by regionally enhancing IFN-gamma production. Clin Cancer Res, 2013; 19, 668-79.
4. Zhang Q, Xu X, Yuan Y, et al. IPS-1 plays a dual function to directly induce apoptosis in murine melanoma cells by inactivated Sendai virus. Int J Cancer, 2014; 134, 224-34.
5. Zhang Q, Zhu H, Xu X, et al. Inactivated Sendai virus induces apoptosis and autophagy via the PI3K/Akt/mTOR/p70S6K pathway in human non-small cell lung cancer cells. Biochem Biophys Res Commun, 2015; 465, 64-70.
6. Kawaguchi Y, Miyamoto Y, Inoue T, et al. Efficient eradication of hormone-resistant human prostate cancers by inactivated Sendai virus particle. Int J Cancer, 2009; 124, 2478-87.
7. Gao H, Gong XC, Chen ZD, et al. Induction of apoptosis in hormone-resistant human prostate cancer PC3 cells by inactivated Sendai virus. Biomed Environ Sci, 2014; 27, 506-14.
8. Narantsogt G, Min A, Nam YH, et al. Activation of MAPK Is Required for ROS Generation and Exocytosis in HMC-1 Cells Induced by Trichomonas vaginalis-Derived Secretory Products. Korean J Parasitol, 2015; 53, 597-603.
9. McCubrey JA, Lahair MM, Franklin RA. Reactive oxygen species-induced activation of the MAP kinase signaling pathways. Antioxid Redox Signal, 2006; 8, 1775-89.
10. Tournier C, Hess P, Yang DD, et al. Requirement of JNK for stress-induced activation of the cytochrome c-mediated death pathway. Science, 2000; 288, 870-4.
11. Assefa Z, Vantieghem A, Garmyn M, et al. p38 mitogen-activated protein kinase regulates a novel, caspase-independent pathway for the mitochondrial cytochrome c release in ultraviolet B radiation-induced apoptosis. J Biol Chem, 2000; 275, 21416-21.
12. El-Najjar N, Chatila M, Moukadem H, et al. Reactive oxygen species mediate thymoquinone-induced apoptosis and activate ERK and JNK signaling. Apoptosis, 2010; 15, 183-95.
13. Zhang Q, Wang Z, Yuan Y, et al. Immunoadjuvant effects of hemagglutinating virus of Japan envelope (HVJ-E) on the inactivated H9 subtype avian influenza virus vaccine. Vet Immunol Immunopathol, 2011; 141, 116-23.
14. Leibowitz B, Yu J. Mitochondrial signaling in cell death via the Bcl-2 family. Cancer Biol Ther, 2010; 9, 417-22.
15. Scorrano L, Korsmeyer SJ. Mechanisms of cytochrome c release by proapoptotic BCL-2 family members. Biochem Biophys Res Commun, 2003; 304, 437-44.
16. Deng S, Tang S, Zhang S, et al. Furazolidone induces apoptosis through activating reactive oxygen species-dependent mitochondrial signaling pathway and suppressing PI3K/Akt signaling pathway in HepG2 cells. Food Chem Toxicol, 2015; 75, 173-86.
17. Tanemura A, Kiyohara E, Katayama I, et al. Recent advances and developments in the antitumor effect of the HVJ envelope vector on malignant melanoma: from the bench to clinical application. Cancer Gene Ther, 2013; 20, 599-605.
18. Zheng QS, Zheng RL. Effects of ascorbic acid and sodium selenite on growth and redifferentiation in human hepatoma cells and its mechanisms. Pharmazie, 2002; 57, 265-9.
19. Circu ML, Aw TY. Reactive oxygen species, cellular redox systems, and apoptosis. Free Radic Biol Med, 2010; 48, 749-62.
20. Hao W, Yuan X, Yu L, et al. Licochalcone A-induced human gastric cancer BGC-823 cells apoptosis by regulating ROS-mediated MAPKs and PI3K/AKT signaling pathways. Sci Rep, 2015; 5, 10336.
21. Chetram MA, Bethea DA, Odero-Marah VA, et al. ROS-mediated activation of AKT induces apoptosis via pVHL in prostate cancer cells. Mol Cell Biochem, 2013; 376, 63-71.
22. Ciriolo MR, Palamara AT, Incerpi S, et al. Loss of GSH, oxidative stress, and decrease of intracellular pH as sequential steps in viral infection. J Biol Chem, 1997; 272, 2700-8.
23. Chakraborty S, Mazumdar M, Mukherjee S, et al. Restoration of p53/miR-34a regulatory axis decreases survival advantage and ensures Bax-dependent apoptosis of non-small cell lung carcinoma cells. FEBS Lett, 2014; 588, 549-59.
24. Yuan Y, Wang Y, Hu FF, et al. Cadmium Activates Reactive Oxygen Species-dependent AKT/mTOR and Mitochondrial Apoptotic Pathways in Neuronal Cells. Biomed Environ Sci, 2016; 29, 117-26.
25. Amatore D, Sgarbanti R, Aquilano K, et al. Influenza virus replication in lung epithelial cells depends on redox-sensitive pathways activated by NOX4-derived ROS. Cell Microbiol, 2015; 17, 131-45.